WILEY | Hindawi

Research Article

Hydrodynamic and Geostress Controls on CBM Enrichment in the Anze Block, Southern Qinshui Basin, North China

Dameng Liu [1,2] **Zheng Zhao** [1,2] **Xiaoming Jin,**[1,2] **Chao Yang,**[1,2] **Wei Chen,**[3] **Yidong Cai** [1,2] **Yongkai Qiu,**[1,2] **Yuejian Lu** [1,2] **and Yingfang Zhou** [4]

[1]*School of Energy Resources, China University of Geosciences, Beijing 100083, China*
[2]*Coal Reservoir Laboratory of Natural Engineering Research Center of CBM Development & Utilization, China University of Geosciences, Beijing 100083, China*
[3]*Beijing Furuibao Energy Technology Company, Beijing 100176, China*
[4]*School of Engineering, Fraser Noble Building, King's College, University of Aberdeen, AB24 3UE Aberdeen, UK*

Correspondence should be addressed to Dameng Liu; dmliu@cugb.edu.cn

The coalbed methane (CBM) resource in the southern Qinshui Basin, North China, is abundant. Proper understanding of the geological control factors on CBM enrichment in Anze Block of southern Qinshui Basin is critical to design efficient CBM development plan in this area. Field and laboratory data including well logging, well testing, hydraulic fracturing, and groundwater chemical analysis of were used to evaluate the characteristics of the hydrodynamic and geostress, and then, the combined effect of hydrodynamic and geostress field on CBM enrichment was analyzed. The results show that the total dissolved solids (TDS) of groundwater in the west is generally lower than that in other areas in the block, and the primary formation water is $NaHCO_3$-type. The geostress field shows a $\sigma_H > \sigma_v > \sigma_h$ dominated geostress type in this area, and the western block has a lower value than the eastern block. The strong hydrodynamic field with low TDS also has a lower gas content while the weak hydrodynamic field with high TDS has a higher gas content. Both the TDS value and the horizontal stress differences are positively related to the gas content, indicating that inactive hydrodynamics and large horizontal stress difference of coal reservoir is favorable for CBM preservation.

1. Introduction

Identifying the distribution characteristics of coalbed methane (CBM) is one of the main objectives of CBM resource exploration and an essential guarantee for efficient CBM development [1]. The study of the effect of the main geological factors on the CBM enrichment is the basis for evaluating the distribution characteristics of CBM resources. Based on the analysis of a large amount of exploration and development data, tectonic conditions, coal seam burial depth, hydrogeological conditions, depositional environment, and coal seam physical properties were considered as the main geological factors that affect CBM resource enrichment [2–4]. Among them, the influence of hydrodynamic field on CBM enrichment was investigated by groundwater geochemical characterization in coal seams [5] and fluid energy calculations based on specific reservoir parameters [6]. It was concluded that the distribution of methane carbon isotopes in coalbed water is related to the CBM formation [5, 7, 8]. Weak runoff areas with stagnant groundwater have higher salinity and desulfurization coefficients [9], which are easy to form hydrodynamic seal [10] and favorable for CBM enrichment [11, 12]. On the contrary, strong hydrodynamic conditions result in hydrodynamic scour and cause gas loss [13].

Previously in the literature, the geostress distribution were directly tested by arranging borehole stress testing [14] or predicted with geostress models based on logging data, well test data, and hydraulic fracturing data [15–17]. Then, formulate

correlation between geostress and reservoir gas content [18]. It is concluded that high tectonic stress determines the presence of high reservoir pressure and high gas content [19]. A higher vertical stress guarantees a lower possibility of CBM transport and dissipation to the surface, and thus, it is easier to store gas [20].

Anze Block is one of the blocks with high gas content in Qinshui Basin, and there is a significant amount of work focused on geological structure, reservoir permeability, and gas content prediction [21]. However, no systematic research on combined effect of multifield, for example, geostress field and hydrodynamic field, on CBM enrichment in Anze Block has been carried out. In this work, the geostress field, hydrodynamic field, and gas content distributions were evaluated based on geological exploration data and laboratory test data in Anze Block, and the effects of the geostress field, hydrodynamic field, and their combined effect on CBM enrichment was investigated thoughtfully (Figure 1). The research is expected to provide a geological basis for further exploration and development of CBM resources in the Anze Block.

2. Geological Background

2.1. Tectonic Evolutionary Features. The Anze Block is located in the southern part of the Qinshui Basin, Shanxi Province, China, with regional stratigraphic trends to the north-east and gentle production, and stratigraphic tendencies to the south-east, with stratigraphic dips generally in the range of 2° to 12°, to the west by the Huoshan backslope and to the east by the Qinshui complex oblique (Figure 2).

The Anze Block experienced four stages of tectonic evolution. The first stage refers to the north-south extrusive stresses from the Late Hercynian period to Indo-Chinese periods forming WE-oriented folds and increasing the burial depth of coal seams to the maximum burial depth. In the early and middle Yanshan period, the block was mainly dominated by extrusion uplift and folding on account of the Yanshan movement, which formed NE-SW and NNE-SSW trending backward and forward slope. In the late Yanshan period, the crust was in a state of tectonic uplift and uplift, which result in strong denudation in the Anze Block, and the burial depth of coal seam decreased gradually. In the early and late Himalayan period, the structural differentiation was stronger due to the different ground stress character, which is leading to most areas keep stable except some parts of areas were subsided or subsiding slightly.

2.2. Characteristics of the Coal Seam. The main coal-bearing strata consists of Carboniferous Taiyuan Formation and the Permian Shanxi Formation in the Qinshui Basin, which include nos. 3 and 15 coal seams [22–24], and here in this work, we focus on the no. 3 coal seam. The thickness of no.3 coal seam in Anze Block increases along the W-E direction gradually, and the thickest part of the coal seam located in the south and southeast of the study area. No. 3 coal seam has a large thickness in a single layer, and the thickness variation range from 4.5 m to 7.7 m, with an average thickness of 6.77 m. Part of coal seam is divided into upper and lower layers by 1 or 2 gangue layers (as shown in Figure 3). The

porosity of coal seam in the Anze Block varies from 1.91% to 5.44%, with an average porosity of 3.98%. The permeability variation ranges from 0.011 mD to 0.21 mD, with an average permeability of 0.068 mD. The structure of coal seam in the study area is mainly fracture structure. The minimum gas content of no. 3 coal seam is $5.5 \, cm^3/g$, the maximum is $25.2 \, cm^3/g$, and the average gas content is $12.23 \, cm^3/g$.

The roof and floor of coal reservoir are important for affecting the preservation of CBM in coal seams. In the study area, the roof with has strong stability and great thickness is mostly consist of dark gray mudstone, dark gray tight sandstone, and argillaceous sandstone. Meanwhile, the floor lithology is dominated by dark gray sandy mudstone and mudstone. During geological evolution process, the mudstone and argillaceous sandstone normally have low porosity and permeability due to the compaction by diagenesis, which indicates that the overlying strata has good sealing and preservation performance for CBM in the no. 3 coal seam.

3. Hydrodynamic Field Characteristics

3.1. The Chemical Characteristic of Groundwater in Coal Seams. The chemistry characteristics of coal reservoir groundwater include the total dissolved solids (TDS), ion type, hydrogen and oxygen isotopes of water, and microelement and rare-earth elements, which could be used to clarify the groundwater quality, water source, hydrodynamic intensity, and runoff characteristics [5, 25]. In this work, 23 water samples were collected for chemistry characteristics analysis based on the SY/T 5523-2006 standard; the concentration of ions in groundwater was measured with manual titration. All experiments in this work were performed at 25°C, 0.1 MPa, and 30% in relative air humidity. The results of chemistry characteristics in Anze Block are summarized in Table 1. As shown in this table, the primary compositions of water produced from coal reservoir are Ca^{2+}, Mg^{2+}, $Na^+ + K^+$, SO_4^{2-}, Cl^-, and HCO_3^-. The contents of $Na^+ + K^+$, Cl^-, and HCO_3^- are the major components, which vary greatly from well to well (as shown in Table 1) and play an important role in identifying the type, TDS, and intensity of groundwater activity of recovered water from CBM. $Na^+ + K^+$ concentration of the highest of up to 2455.95 mg/L in well A1-2, the minimum concentration is 356.32 mg/L in well A29, and average value is 707.31 mg/L in Anze Block. The maximum concentration value is 3129.80 mg/L for Cl^-, the minimum of it appears in well A21 is 106.09 mg/L, and the average value is 443.10 mg/L. In addition, the highest and lowest concentration of HCO_3^- is 2349.21 mg/L and 630.28 mg/L, respectively, and the average concentration was 1183.03 mg/L. Compared with $Na^+ + K^+$, Cl^-, and HCO_3^-, the concentration of Ca^{2+}, Mg^{2+}, and SO_4^{2-} fluctuated less excluding a handful of outliers in some wells; these outliers may be related to formation structure or lithology around the well.

Figure 4 presents TDS as a function of $Na^+ + K^+$ concentration for the formation water samples. As shown in this figure, the TDS increases linearly with the $Na^+ + K^+$ concentration. TDS of water in CBM wells indicate the total amount of various ions, molecules, and compounds which dissolved in
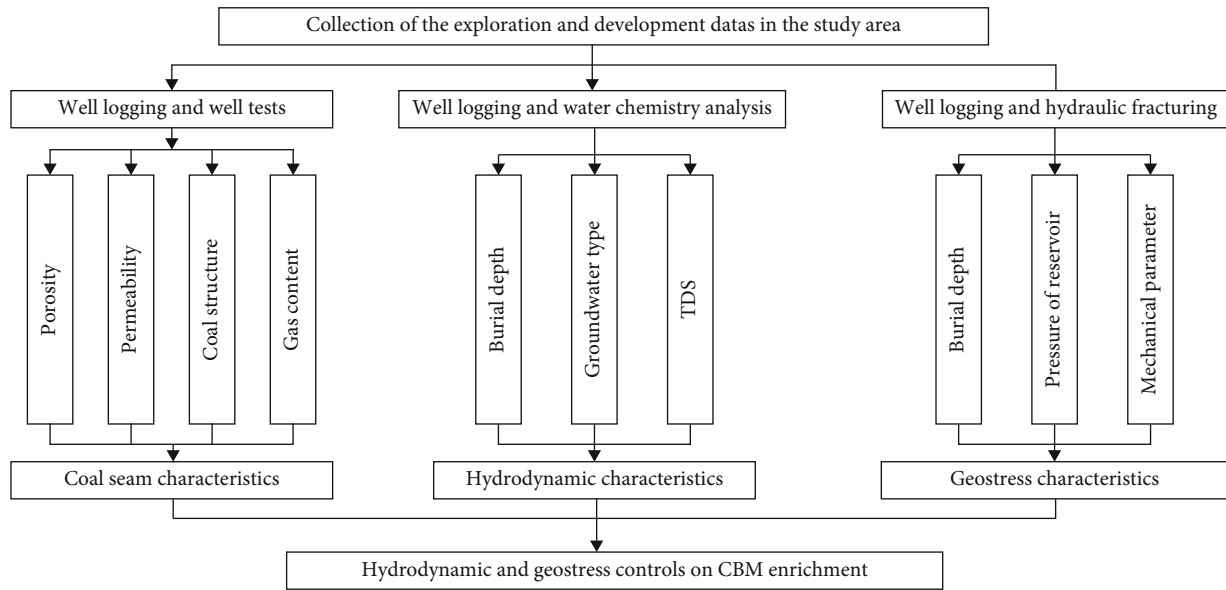
FIGURE 1: The research flow diagram.

water. A wide range of TDS was measured ranging from 1209.93 to 6816.71 mg/L in study area, with an average value of 3064.64 mg/L, which is much lower than that of seawater TDS of 35000 mg/L.

Based on the ion concentration, TDS of water, trilinear diagram (Figure 5(a)), and stiff diagram (Figure 5(b)), there are two types of formation water in the Anze Block, NaCl-type and $NaHCO_3$-type, respectively. According to the previous study, CBM always enriched in stagnant areas where the water is static or moves slowly and is dominated by Na^+ and Cl^- [5, 12], which indicates that the Anze Block is favorable for CBM preservation.

3.2. Groundwater Geochemical Characteristics in Coal Seams. The formation water geochemical characteristics can be evaluated by different parameters, including metamorphic coefficient (Cl-Na coefficient), desulfurization coefficient, Cl-Mg coefficient, Ca-Mg coefficient, and carbonate equilibrium coefficient [5].

The groundwater geochemical parameters in coal seams, obtained from 19 wells in the Anze Block (Figure 6), show that the metamorphic coefficient ranges from 1.23 to 8.01, with a median of 3.35; the desulfurization coefficient ranges from 0.36 to 100.45, with a median of 2.76; the carbonate equilibrium coefficient is in the range of 8.74 to 195.49, with a median of 61.98; the Cl-Mg coefficient ranges from 7.61 to 106.45, with a median of 20.29; and the Ca-Mg coefficient ranges from 0.40 to 3.01, with a median of 1.00. The favorable aeras with rich gas content are characterized by high TDS, Cl-Mg coefficient, low metamorphic coefficient and desulfurization coefficient, low Ca-Mg coefficient, and low carbonate equilibrium coefficient. Meanwhile, TDS, which have a good linear relationship with ion concentration (Figure 4), is also a common geochemical parameter used to evaluate hydrodynamic strength. The strong hydrody-

namic field with TDS more than 2000 mg/L always has a good reservoir preservation condition, while the weak hydrodynamic field with TDS less than 2000 mg/L has a bad reservoir preservation condition.

3.3. Hydrodynamics of Groundwater. The TDS of groundwater in coal seams, which is the result of long-term evolution of rock strata and groundwater, reflects the concentration characteristics of major ionic components and is also an important indicator for researching the hydrochemistry of the formation. Thus, the TDS could be used to characterize the hydrodynamics of groundwater [3]. Previous study shows that the Cl^-, Na^+, and K^+ contents in the study area are low, and the water type is dominated by SO_4-HCO_3-Ca-Mg-type. In the strong runoff area, the water type is dominated by Ca-SO_4 or Mg-SO_4. For stagnant area, the water type is $NaHCO_3$-type or NaCl-type [5].

The TDS of groundwater in Anze Block is relatively low with range from 1209.93 mg/L to 6816.71 mg/L, and the overall trend shows that the western part is lower than the eastern part, the southern and northern parts are relatively higher, and the central region is lower in general (see Figure 7(b)). According to the TDS distribution characteristics, the study area could be divided into three parts, including runoff area, stagnant area, and transition area (weak runoff area). Runoff area is in the western part of the study area, stagnant area is located in the northeastern and parts of the southern, and transition area is in the central region. Meanwhile, the flow direction of groundwater in the study area is roughly from the west to the east, as presented in Figure 7(b). Runoff area would be formed due to the flow from the both sides in the north and south directions and then further formed stagnant area, that is, the flow direction of groundwater is from the runoff area to stagnant area.
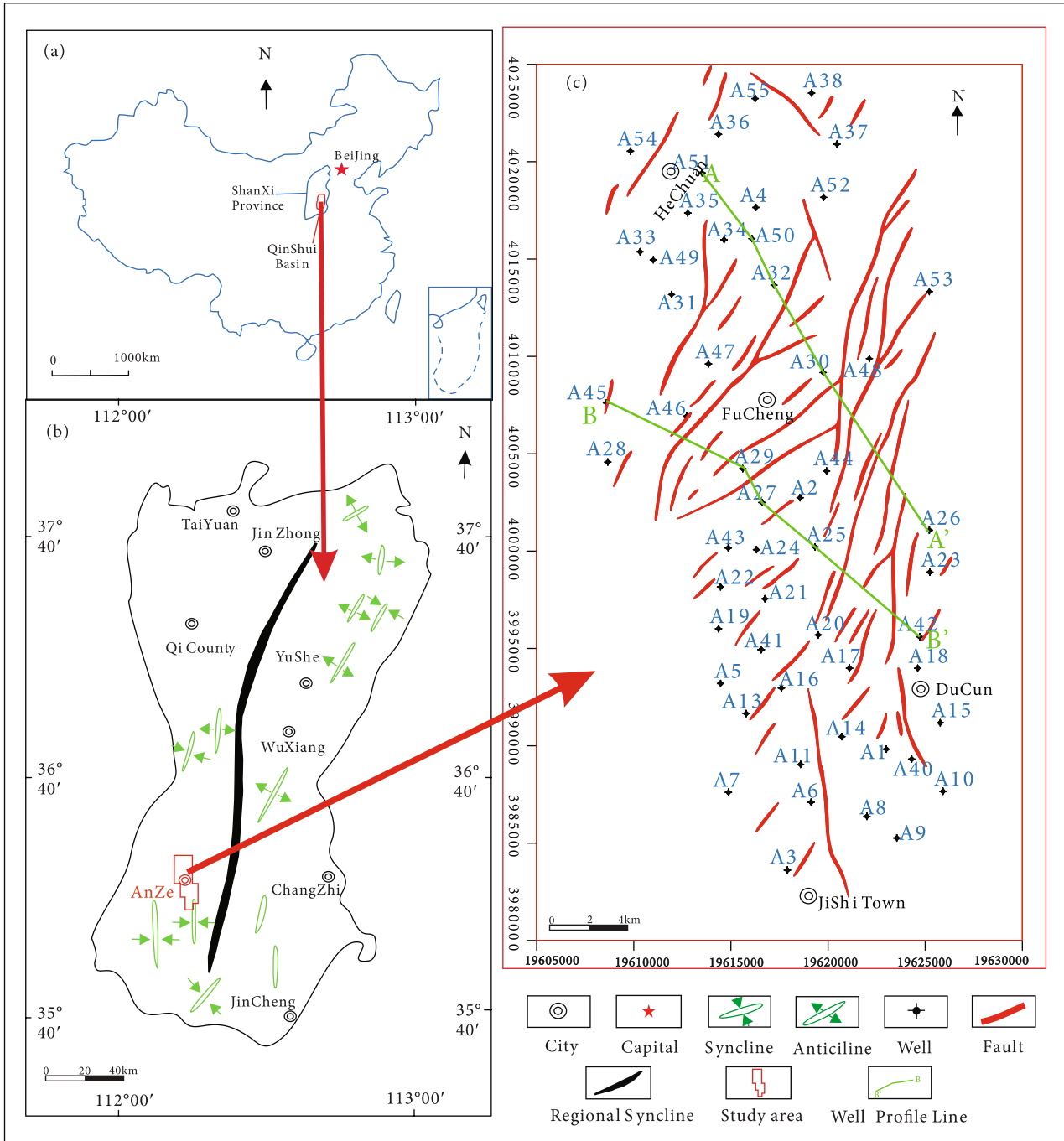
FIGURE 2: The location and geological structure of Anze Block, southern Qinshui Basin, Shanxi Province, China. (a) The location of Qinshui Basin. (b) The geological structure of the Qinshui Basin. (c) The geological structure of the Anze Block.

4. Geostress Characteristics

4.1. Calculation of Geostress. The Anderson in situ stress model is widely used to study geostress; in this model, tectonic stress generated horizontally is proportional to the pressure of the overlying rock layer [26, 27], and the model is chosen for this study to investigate the geostress distribution in the Anze Block. Which could be written as follows:

$$\sigma_h = \left(\frac{\mu}{1 - \mu} + \beta_h \right) \left(\sigma_v - \alpha p_p \right) + \alpha p_p, \tag{1}$$

$$\sigma_H = \left(\frac{\mu}{1 - \mu} + \beta_H \right) \left(\sigma_v - \alpha p_p \right) + \alpha p_p, \tag{2}$$

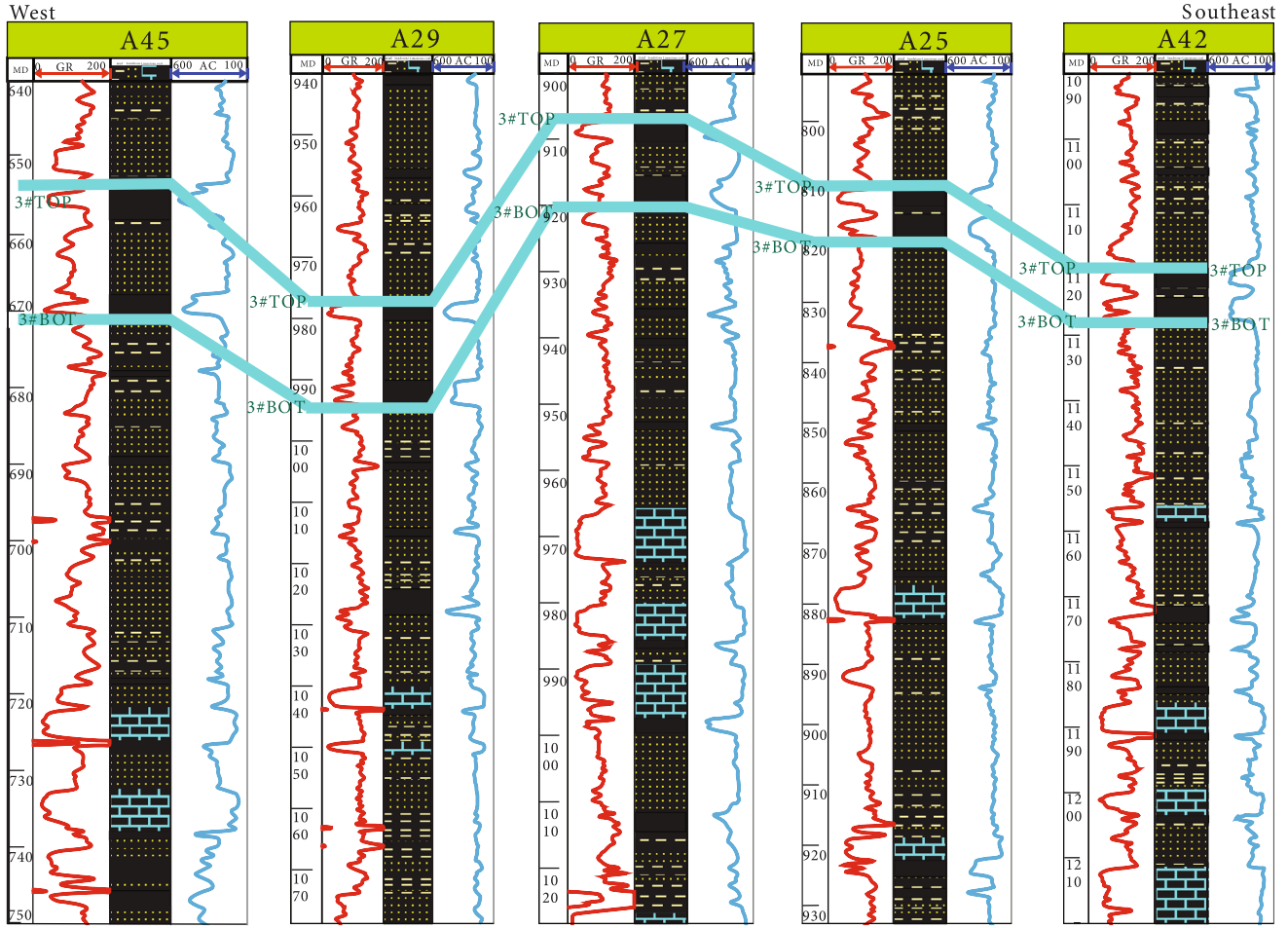where σ_h and σ_H are the minimum and maximum horizontal

Figure 3: The profile of well-connection in the Anze Block (well A45, A29, A27, A25, and A42, left to right).

geostresses, respectively, MPa. σ_v is the vertical geostress, MPa. μ is the Poisson's ratio of the rock. α is the biot factor. p_p is the pressure of reservoir, MPa. β_h and β_H are the minimum and maximum horizontal geostress tectonic factor, respectively.

The vertical stress is usually calculated from the gravity of the overlying strata, and in the study area, its estimation equation can be expressed as

$$\sigma_v = 0.27h, \tag{3}$$

where h is the thickness of the overlying strata (or burial depth), m.

Combining the geostress parameters of some known wells in the study area and the Anderson in situ stress model, the minimum and maximum horizontal geostress tectonic factor can be inferred (Table 2), and the results show that β_h varies from -0.1395 to 0.4791, with the average of 0.1482, and the β_H varies from 0.1966 to 1.8286, with the average of 0.7599. The model for calculating geostress in this study area could be expressed as:

$$\sigma_h = \left(\frac{\mu}{1-\mu} + 0.1482 \right) \left(\sigma_v - \alpha p_p \right) + \alpha p_p, \tag{4}$$

$$\sigma_H = \left(\frac{\mu}{1-\mu} + 0.7599 \right) \left(\sigma_v - \alpha p_p \right) + \alpha p_p. \tag{5}$$

4.2. Distribution Characteristics of Geostress. The calculation (Figure 8) shows that the minimum horizontal principal stress of no. 3 coal seam is in the range of 7.31 to 24.90 MPa in the study area, with an average of 18.93 MPa; the maximum horizontal principal stress of coal seam ranges from 17.88 to 40.64 MPa, with an average of 31.89 MPa; the vertical geostress is in the range of 14.93 to 32.74 MPa, with an average of 24.36 MPa. The average of geostress is greater than 18 MPa in the Anze Block, that is, study area belongs to relatively high stress zone.

The vertical geostress in Anze Block shows a trend of low in the west and high in the east as presented in Figure 8(a). The distribution of the minimum and maximum horizontal principal stresses is similar to that of vertical geostress (see Figures 8(b) and 8(c)), and the horizontal stress values basically extend along the burial depth contour of coal seam. Due to the development of faults in the area [27], the

TABLE 1: The ion concentration and TDS of groundwater in Anze Block.

| Sample ID | Concentration of different ions (mg/L) | | | | | | TDS (mg/L) | Water type |
	$Na^+ + K^+$	Mg^{2+}	Ca^{2+}	Cl^-	SO_4^{2-}	HCO_3^-		
A1-1	1584.44	21.50	35.46	1556.06	18.89	1718.93	4935.28	NaCl
A1-2	2455.95	14.33	3.94	3129.80	9.44	1203.25	6816.71	NaCl
A1-3	2360.18	4.78	3.94	2776.15	160.53	1317.85	6623.43	NaCl
A4	492.86	4.78	3.94	141.46	9.44	1088.66	1741.14	NaHCO$_3$
A4-1	1575.66	14.33	11.82	1838.98	28.33	1088.66	4557.78	NaCl
A4-2	1247.02	2.39	7.88	1237.77	9.44	1203.25	3707.75	NaCl
A4-3	1685.62	11.94	7.88	1892.02	9.44	1289.20	4896.10	NaCl
A6	745.76	16.72	35.46	389.01	9.44	1489.74	2686.13	NaHCO$_3$
A8	702.73	11.94	59.1	300.60	9.44	1575.69	2659.50	NaHCO$_3$
A10	636.55	4.78	7.88	229.87	18.89	1317.85	2215.82	NaHCO$_3$
A14	474.84	4.78	7.88	353.65	9.44	687.57	1538.16	NaHCO$_3$
A15	734.85	2.39	3.94	141.46	9.44	1718.93	2611.01	NaHCO$_3$
A21	388.10	2.39	3.94	106.09	9.44	859.47	1369.43	NaHCO$_3$
A23	1187.17	4.78	7.88	1485.33	9.44	630.28	3324.88	NaCl
A24	469.93	4.78	3.94	106.09	9.44	1088.66	1682.84	NaHCO$_3$
A29	356.32	2.39	3.94	141.46	75.54	630.28	1209.93	NaHCO$_3$
A31	432.14	4.78	3.94	247.55	9.44	744.87	1442.72	NaHCO$_3$
A33	1153.42	4.78	3.94	530.47	727.09	1260.55	3680.25	NaHCO$_3$
A35	753.23	4.78	3.94	742.66	9.44	744.87	2258.92	NaCl
A39	389.45	2.39	3.94	141.46	9.44	802.17	1348.85	NaHCO$_3$
A41	1259.00	2.39	3.94	583.52	9.44	2349.21	4207.50	NaHCO$_3$
A48	568.55	2.39	3.94	176.82	245.51	916.76	1913.97	NaHCO$_3$
A53	848.35	4.78	3.94	689.62	9.44	1088.66	2644.79	NaCl
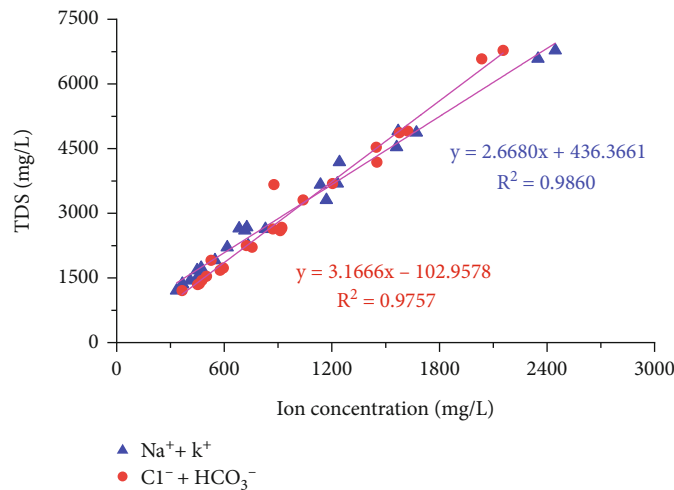
FIGURE 4: Relationship between $Na^+ + K^+$ and $Cl^- + HCO_3^-$ concentration and TDS.

horizontal stress in the central part is relatively low. The overall trend of geostress in the study area is low in the west and high in the east, and the south and north are higher than the central area.

The minimum horizontal stresses, maximum horizontal stresses, and vertical stresses vs. the burial depth of the coal seam is presented in Figure 9(a). As shown in this subfigure, positive correlation is observed within the margin of
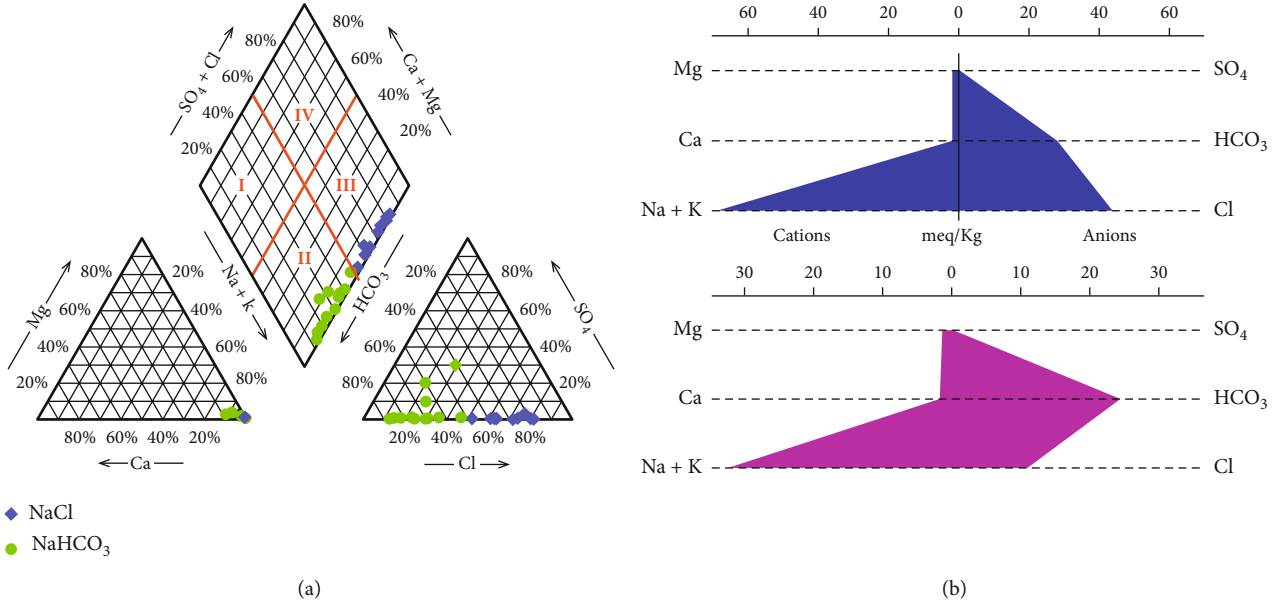
FIGURE 5: Water chemical characteristics of coal reservoir in Anze Block. (a) Piper trilinear diagram of water chemistry. (b) Stiff water pattern diagram of water.

experimental error, indicating that the burial depth of the coal seam has great effect on the stress distribution and value. The lateral pressure coefficient k, which is used to describe the state of ground stress at a point, is the ratio of the average of the minimum and maximum horizontal principal stress to the vertical stress and is calculated as follows:

$$k = \frac{\sigma_h + \sigma_H}{2\sigma_v}. \tag{6}$$

As shown in Figure 9(b), the lateral pressure coefficient is opposite to the extension direction of the burial depth contour of coal seam, that is, it decreasing with the increase of the coal seam depth. The lateral pressure coefficients of the Anze Block were fitted with reference to Hoek-Brown model [28], and the linear equations were obtained as follows:

$$\left(\frac{100}{H} + 0.45\right) < k < \left(\frac{400}{H} + 0.9\right). \tag{7}$$

The geostress in the area is mainly dominated by $\sigma_H > \sigma_v > \sigma_h$ type based on the distribution of lateral pressure coefficients in the Anze Block as shown in Figure 9(a). The coal reservoir is in compression state, which is favorable to CBM production. A part of areas where the coal seam is buried at a shallow depth (650-750 m) develop horizontal fractures, which has a negative effect on the escape of CBM from the coal reservoir.

The lateral pressure coefficient of the Anze Block (Fitting envelope) is between the Hoek-Brown envelope and Chinese envelope and is generally distributed close to the Chinese inner envelope (see Figure 9(b)). The lateral pressure coefficient shows a general trend of decreasing with deeper coal

seam burial, but this trend is not very obvious. The individual discrete points that appear are likely due to the shallow coal seams being affected by fault fractures and tectonic activity.

5. Hydrodynamics and Geostress Control on CBM Enrichment

5.1. The Distribution of Gas Content. According to the distribution range of gas content in the study area, it can be divided into three types: low gas content areas with the gas content less than $10 \, \text{cm}^3/\text{g}$; middle gas content areas with the gas content between 10 and $20 \, \text{cm}^3/\text{g}$; high gas content areas with the gas content greater than $20 \, \text{cm}^3/\text{g}$. Meanwhile, the hydrodynamic field of the coal reservoir in the study area could be divided into two types based on the effect of TDS on the reservoir preservation conditions. Strong dynamic field, where the groundwater activity of the coal reservoir is active and has a scouring effect on the CBM, is classified by the criterion of TDS < 2000 mg/L. Weak dynamic field, where the groundwater activity of the coal seam is inactive, is classified by the criterion of TDS < 2000 mg/L.

The flow direction of groundwater is from the shallow part of coal seam with low burial depth to the high burial depth or from the strong dynamic field to the weak dynamic field as shown in Figure 10, and the values of TDS are affected due to the flow and accumulation of groundwater. High TDS of groundwater characterizes for whole study area especially around wells A1, A4, and A40; the TDS value is above 3000 mg/L. Meanwhile, the groundwater of coal reservoir is mainly dominated by $NaHCO_3$-type water, representing a relatively close hydrodynamic environment, and in a reducing environment, which is favorable for preservation and enrichment of CBM. The gas content of these high
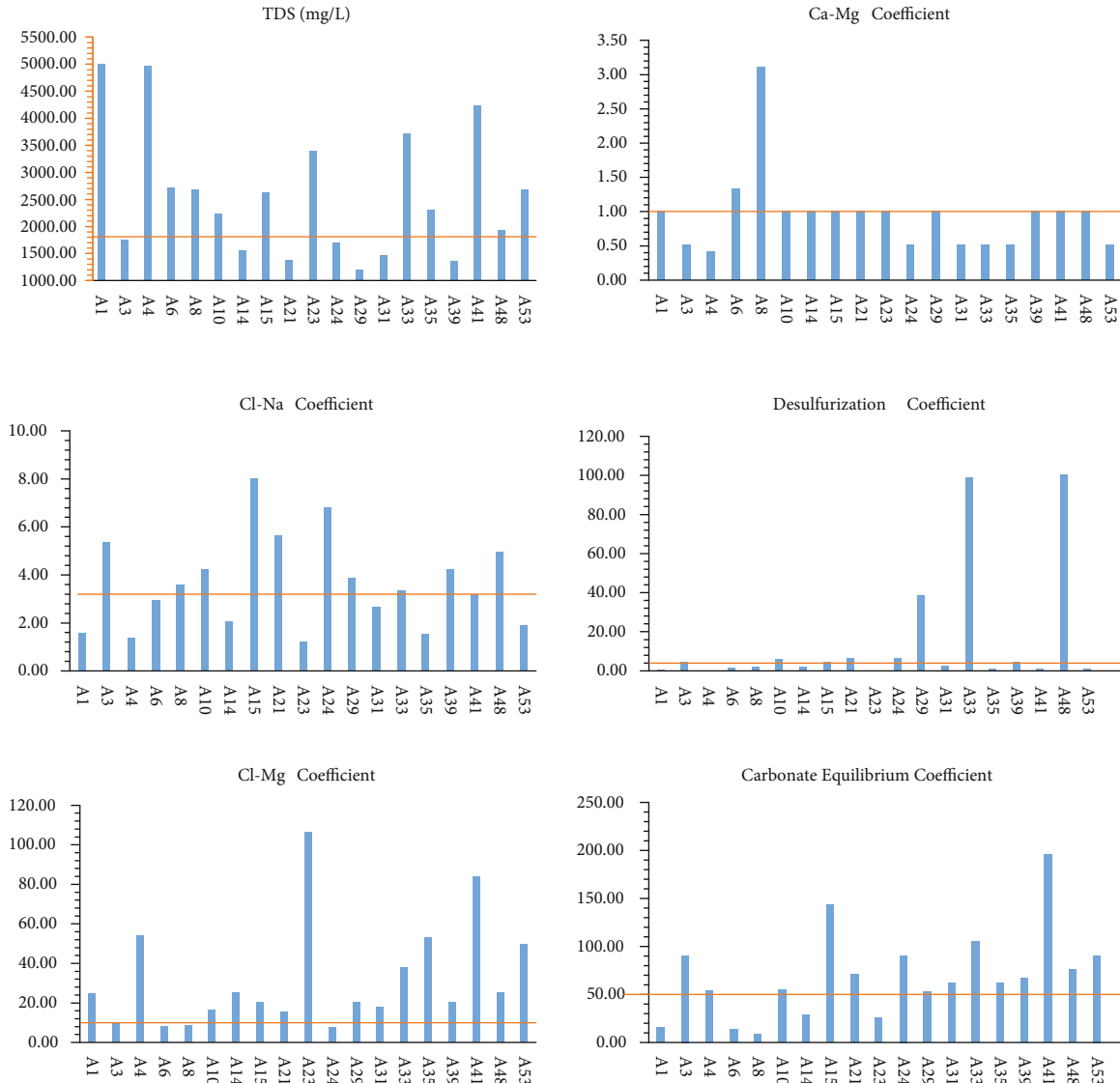
FIGURE 6: Geochemical parameters of groundwater in coal seams.

TDS areas is also relatively high (see Figure 10). The gas content of well A1 is 15.08 cm^3/g and that of well A4 is 17.48 cm^3/g, both of which are in the medium gas content area, while the gas content of well A40 is 25.25 cm^3/g, indicating that there is a weak dynamic field and a reducing environment in the high TDS area, and the high TDS area is beneficial to CBM preservation.

The horizontal stress difference in the study area could be divided into two different areas based on the effect of the horizontal stress difference on the gas content. The low stress area with horizontal stress difference is lower than 13 MPa and the high stress area with horizontal stress difference is higher than 13 MPa. According to the distribution of gas content and geostress shown in Figure 11, the horizontal stress difference decreases gradually along the west to the east direction, which is consistent with burial depth of coal seam. The central part of the study area is tectonically complicated, and the fault is developed well, which leads to frequently changed and ununi-

formed distribution of horizontal stress difference in the central part of the study area. There is a similar changing rule of the horizontal stress difference and the gas content of coal reservoir in the study area, and the two show a positive correlation, that is, as the value of horizontal stress difference of coal reservoir increases, the gas content increases, which may result from a good adsorption capacity for CBM improved due to the reservoir stress increment.

5.2. The Combined Effect of Hydrodynamics and Geostress. The hydrodynamic field has an important influence on the fluid pressure, composition of CBM, and groundwater type in the coal seam; it controls the distribution of gas content through the "recharge-runoff-discharge" hydrodynamic system [5, 6]. The hydrodynamic field may have positive or negative effects on the CBM enrichment. On the one hand, hydraulic dissipation will destroy the gas reservoir in the runoff area. One the other hand, hydraulic sealing has a
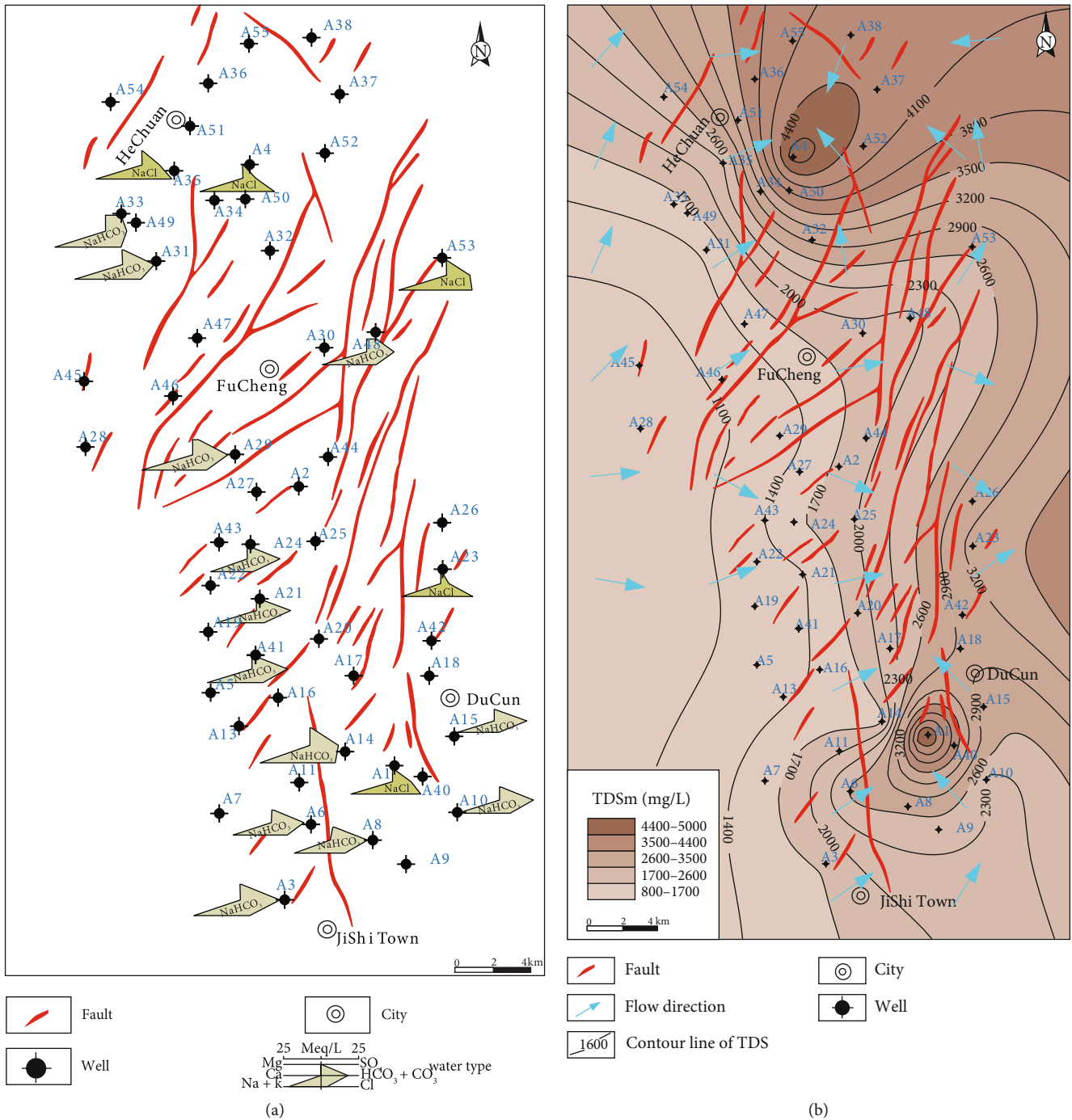
Figure 7: Distribution of groundwater chemical in Anze Bock. (a) Diagram of groundwater type in Anze Block and (b) diagram of groundwater TDS and flow direction in Anze Block.

protective effect on the CBM reservoir in the stagnant area [10, 13].

Geostress is a criterion which indicates the amount of driving energy in coal reservoirs, which not only plays a controlling role in the process of CBM generation but also affects the development of CBM. Geostress has an important influence on the reservoir physical property such as coal structure, permeability, and pore-fracture morphology [29–31]. Generally, areas with relatively high geostress also have relatively high gas content

of coal reservoir. Various tectonic stress and their internal stress distributions would result in changes in the property of coal reservoir, capping layers, and groundwater runoff conditions during the formation of different types of geological structure, which would further affect the content of CBM [19].

Figure 11 shows the coupling effect of hydrodynamic field and geostress field. As shown in this figure, the high gas content area is mainly distributed in the coupled area of weak hydrodynamic field and high horizontal stress difference field,

TABLE 2: Inversion for geostress parameters based on hydraulic fracturing data in the Anze Block.

| Well	Burial depth/m	p_p/MPa	σ_h/MPa	σ_H/MPa	σ_v/MPa	β_h	β_H
A3	863.25-870.80	8.00	19.79	29.46	23.31	0.2300	0.7322
A11	553.30-559.00	3.62	14.83	24.87	14.94	0.3792	1.1016
A14	848.85-855.45	5.08	17.39	27.60	22.92	0.1485	0.6363
A23	1114.10-1121.40	9.53	24.90	38.87	30.08	0.1610	0.6258
A24	891.00-901.00	5.26	16.92	27.35	24.06	0.0176	0.4790
A26	1145.60-1154.30	7.25	17.61	27.68	30.93	-0.1395	0.1966
A35	917.85-930.15	7.06	20.42	31.55	24.78	0.1963	0.6832
A39	731.30-738.45	5.04	19.45	33.51	19.75	0.4791	1.8286
A42	1119.90-1127.80	8.27	19.80	31.14	30.24	-0.0256	0.3941
A50	962.35-937.00	7.52	20.72	33.08	25.98	0.0355	0.9213
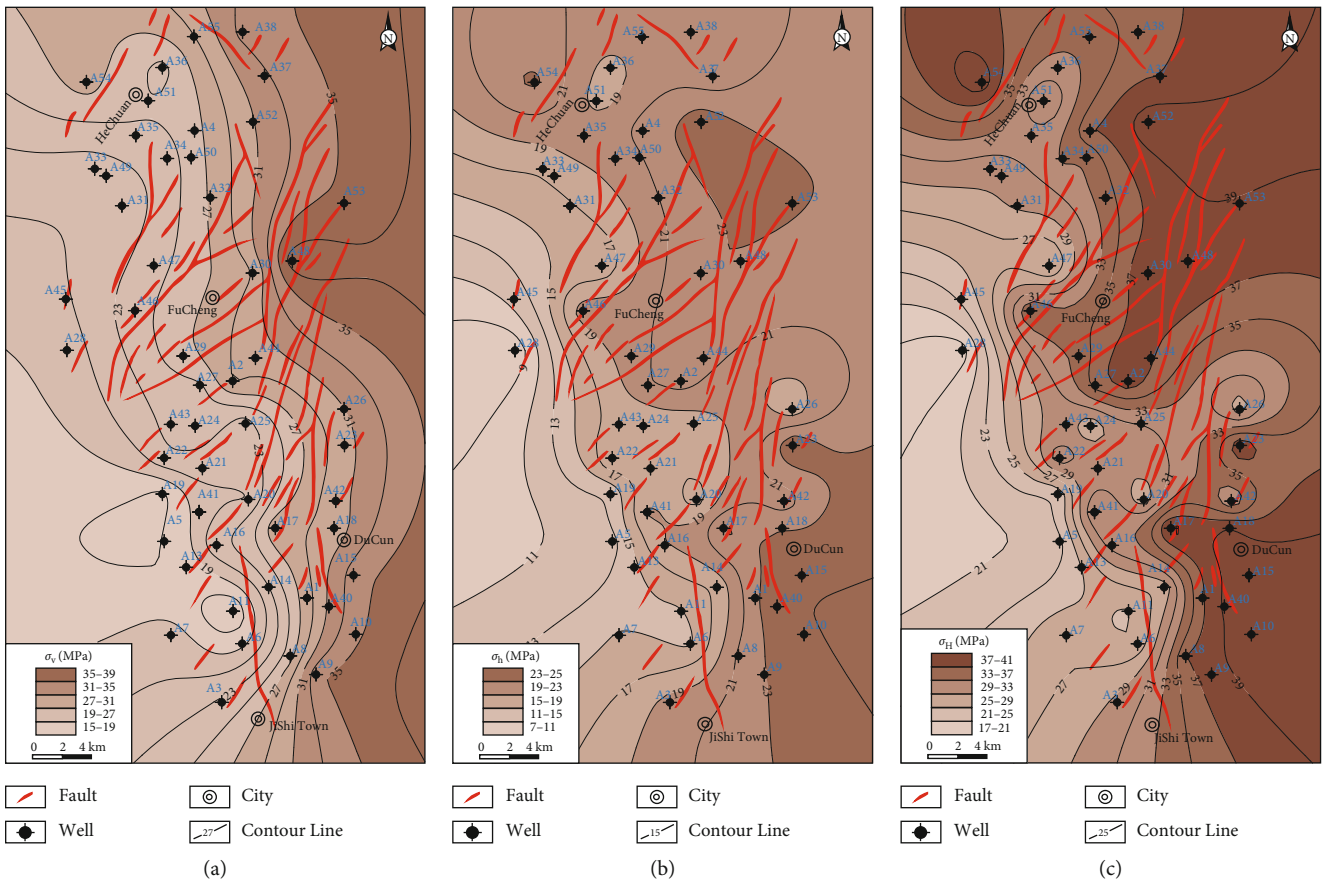
FIGURE 8: Distribution of geostress in Anze Block. (a) Vertical stresses, (b) minimum horizontal principal stresses, and (c) maximum horizontal principal stresses.

while the gas content of coal reservoir is low where the hydrodynamic is strong or the horizontal stress difference is small. The burial depth of coal seam is shallow in the area with strong groundwater hydrodynamic, which has less vertical geostress as well as less reservoir pressure, leads to a lower adsorption capacity of the coal reservoir for CBM and a lower gas content, thus, it is not conducive to CBM enrichment, while in the stagnant area with inactive groundwater, the horizontal stress difference of the coal reservoir is large, and the hydrodynamic activity is small; in addition, the higher geostress promotes the increase of the CBM adsorption capacity of coal reservoirs, which is favorable for CBM enrichment (Figure 11). Therefore, areas with low TDS value indicate that a relatively open hydrodynamic environment and low horizontal stress difference are not conducive to CBM preservation and have low coalbed gas content. On the contrary, inactive hydrodynamic environment is favorable for CBM preservation.
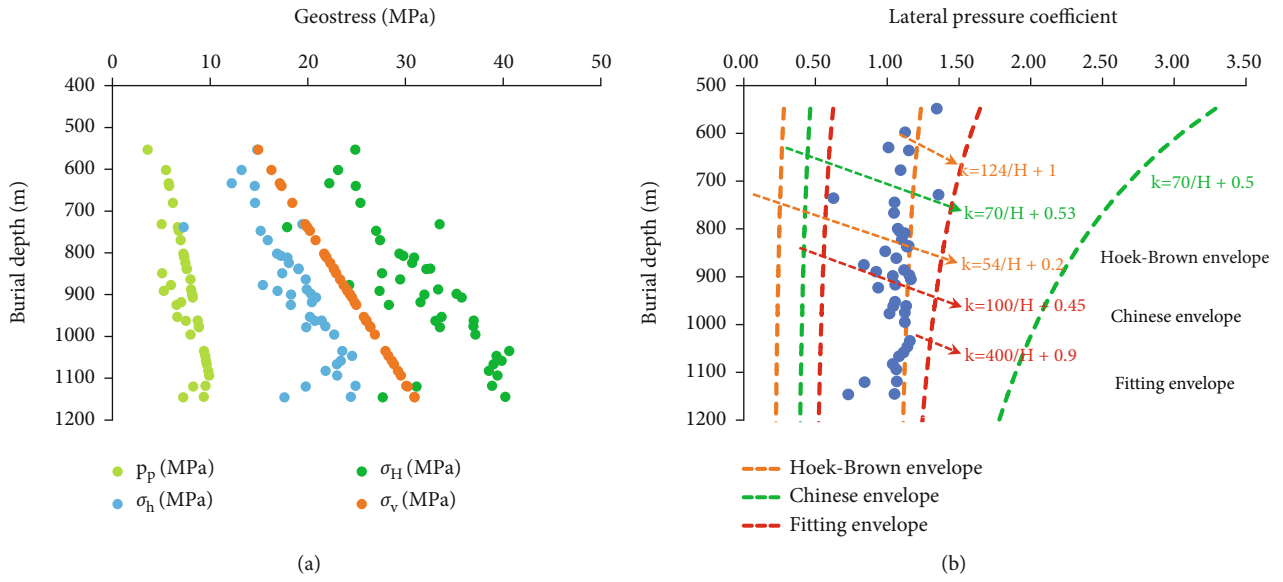
FIGURE 9: Characteristics of the variation of geostress with depth. (a) Different stresses versus depth of burial and (b) lateral pressure coefficient versus depth of burial.
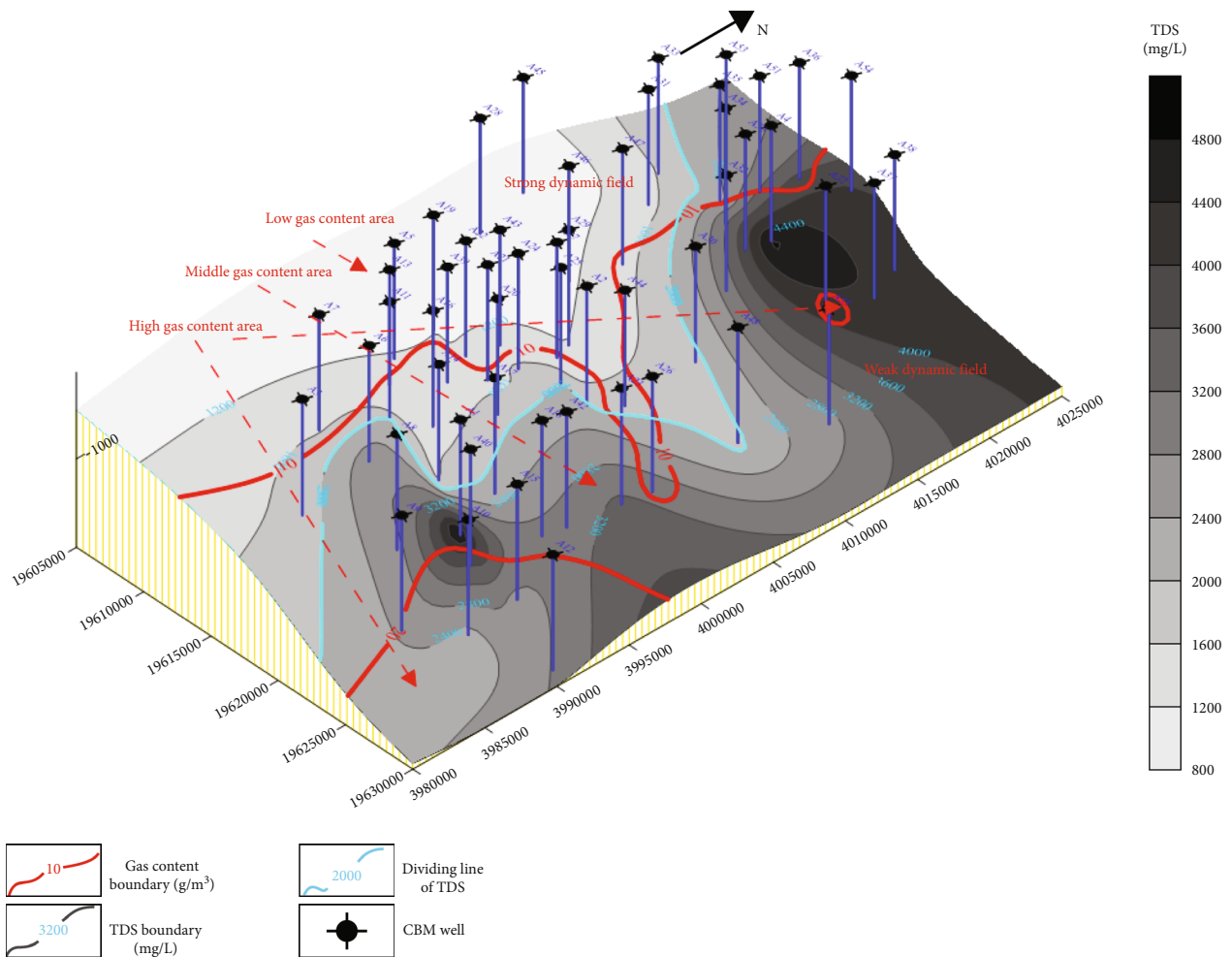

FIGURE 10: The distribution of CBM content under the effect of hydrodynamic field.
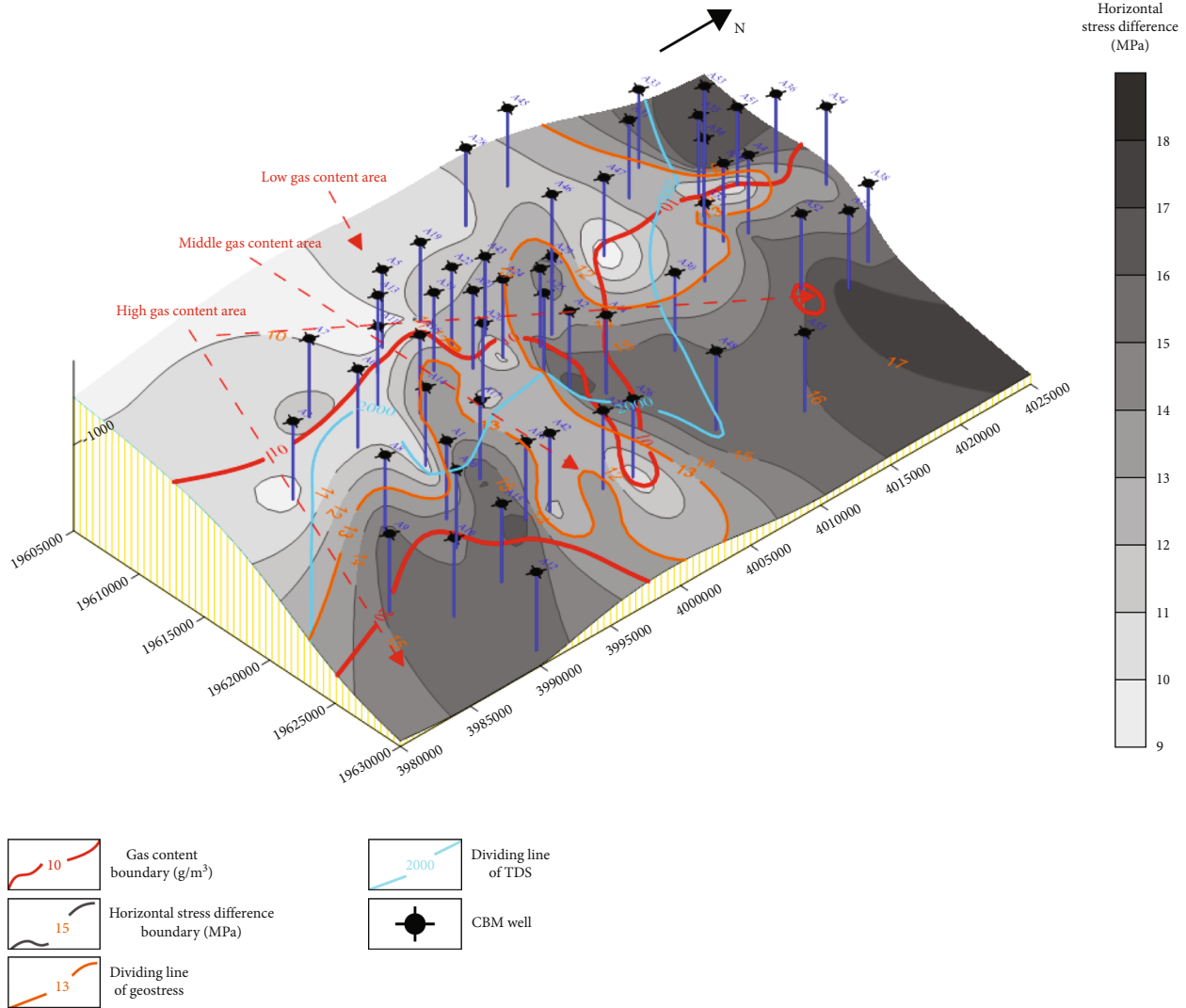
FIGURE 11: The distribution of CBM content under the combined effect of hydrodynamic field and geostress field.

6. Conclusions

Based on well logging, well testing, and water chemistry analysis data of Anze Block, the distribution of hydrodynamic field and geostress field was studied. Meanwhile, the influence of the combined effect of hydrodynamic field and geostress field on CBM enrichment was analyzed. The following conclusions can be reached based on our study:

(1) The TDS of groundwater ranges from 1209.93 to 6816.71 mg/L for no. 3 coal seam in the Anze Block; the western block is generally lower than other parts of the block. In addition, the study area could be divided into runoff area, weak runoff area, and stagnant area three parts, and the water type is mainly dominated by NaCl-type and NaHCO$_3$-type

(2) The maximum horizontal principal stress, the minimum horizontal principal stress, and the vertical stress range from 17.88 to 55.75 MPa, 7.31 to 24.90 MPa, and 14.93 to 32.74 MPa, respectively. The geostress field in the western block is lower and higher in the eastern block, and the geostress in the area is mainly dominated by $\sigma_H > \sigma_v > \sigma_h$ type

(3) The combined effect of hydrodynamic field and geostress field controls the CBM enrichment in Anze Block. The runoff area with low TDS also has a low gas content while the stagnant area with high TDS has a high gas content, and the horizontal stress differenced is positively related to the gas content. The results demonstrate that inactive hydrodynamics and large horizontal stress difference of coal reservoir indicate a favorable CBM preservation area

Data Availability

The data that support the findings of this study are available on request from the corresponding author Dameng Liu.

Conflicts of Interest

The authors declare that they have no conflicts of interest.

Acknowledgments

References

[1] H. Liu, S. Sang, G. Wang, Y. Li, M. Li, and S. Liu, "Evaluation of the synergetic gas-enrichment and higher-permeability regions for coalbed methane recovery with a fuzzy model," *Energy*, vol. 39, no. 1, pp. 426–439, 2012.

[2] X. Zhao, Y. Yang, F. Sun et al., "Enrichment mechanism and exploration and development technologies of high coal rank coalbed methane in south Qinshui Basin, Shanxi Province," *Petroleum Exploration and Development*, vol. 43, no. 2, pp. 332–339, 2016.

[3] H. Fu, D. Tang, T. Xu et al., "Preliminary research on CBM enrichment models of low-rank coal and its geological controls: a case study in the middle of the southern Junggar Basin, NW China," *Marine and Petroleum Geology*, vol. 83, pp. 97–110, 2017.

[4] O. Esen, S. Ozer, A. Soylu, A. Rend, and A. Fisne, "Geological controls on gas content distribution of coal seams in the Kunuk coalfield, Soma Basin, Turkey," *International Journal of Coal Geology*, vol. 231, article 103602, 2020.

[5] Y. Bao, C. An, C. Wang, C. Guo, and W. Wang, "Hydrogeochemical characteristics and water-rock interactions of coalbed-produced water derived from the Dafosi biogenic gas field in the southern margin of Ordos Basin, China," *Geofluids*, vol. 2021, Article ID 5972497, 13 pages, 2021.

[6] Z. Zhang, Y. Qin, Z. Yang, J. Jin, and C. Wu, "Fluid energy characteristics and development potential of coalbed methane reservoirs with different synclines in Guizhou, China," *Journal of Natural Gas Science and Engineering*, vol. 71, article 102981, 2019.

[7] K. Zhang, Z. Meng, and X. Wang, "Distribution of methane carbon isotope and its significance on CBM accumulation of no. 2 coal seam in Yanchuannan CBM block, Ordos Basin, China," *Journal of Petroleum Science and Engineering*, vol. 174, pp. 92–105, 2019.

[8] M. Du, X. Yao, S. Zhang, H. Zhou, C. Wu, and J. Zhao, "Geochemical characteristics and productivity response of produced water from coalbed methane wells in the Yuwang Block, eastern Yunnan, China," *Geofluids*, vol. 2020, Article ID 5702031, 11 pages, 2020.

[9] B. Wang, F. Sun, D. Tang, Y. Zhao, Z. Song, and Y. Tao, "Hydrological control rule on coalbed methane enrichment and high yield in FZ Block of Qinshui Basin," *Fuel*, vol. 140, pp. 568–577, 2015.

[10] Y. Tang, F. Gu, X. Wu, H. Ye, Y. Yi, and M. Zhong, "Coalbed methane accumulation conditions and enrichment models of Walloon Coal measure in the Surat Basin, Australia," *Natural Gas Industry B*, vol. 5, no. 3, pp. 235–244, 2018.

[11] W. Kaiser, D. Hamilton, A. Scott, R. Tyler, and R. Finley, "Geological and hydrological controls on the producibility of coalbed methane," *Journal of the Geological Society*, vol. 151, no. 3, pp. 417–420, 1994.

[12] S. Chen, S. Tao, W. Tian, D. Tang, B. Zhang, and P. Liu, "Hydrogeological control on the accumulation and production of coalbed methane in the Anze Block, southern Qinshui Basin, China," *Journal of Petroleum Science and Engineering*, vol. 198, article 108138, 2021.

[13] B. Wang, B. Jiang, L. Liu et al., "Physical simulation of hydrodynamic conditions in high rank coalbed methane reservoir formation," *Mining Science and Technology*, vol. 19, no. 4, pp. 435–440, 2009.

[14] X. Wang, Q. Hu, and Q. Li, "Investigation of the stress evolution under the effect of hydraulic fracturing in the application of coalbed methane recovery," *Fuel*, vol. 300, article 120930, 2021.

[15] M. Talebi, S. Heidari, M. Moosavi, and M. Rahimi, "In situ stress measurements of two hydropower projects in Iran by hydraulic fracturing method," *Arabian Journal of Geosciences*, vol. 8, no. 9, pp. 7073–7085, 2015.

[16] S. Serdyukov, M. Kurlenya, and A. Patutin, "Hydraulic fracturing for in situ stress measurement," *Journal of Mining Science*, vol. 52, no. 6, pp. 1031–1038, 2016.

[17] W. Ju, Z. Yang, Y. Qin, T. Yi, and Z. Zhang, "Characteristics of in-situ stress state and prediction of the permeability in the Upper Permian coalbed methane reservoir, western Guizhou region, SW China," *Journal of Petroleum Science and Engineering*, vol. 165, pp. 199–211, 2018.

[18] B. Sun, D. Lv, Z. Pan, and H. Lian, "Study on reservoir properties and critical depth in deep coal seams in Qinshui Basin, China," *Advances in Civil Engineering*, vol. 2019, Article ID 1683413, 7 pages, 2019.

[19] S. Chen, D. Tang, S. Tao, Z. Chen, H. Xu, and S. Li, "Coal reservoir heterogeneity in multicoal seams of the Panguan syncline, western Guizhou, China: implication for the development of superposed CBM-bearing systems," *Energy & Fuels*, vol. 32, no. 8, pp. 8241–8253, 2018.

[20] Y. Huang, Y. Yang, Y. Yu, Q. Wang, S. Shi, and D. Wang, "Analysis of tectonic stress field in Baode Block and its application in coalbed methane exploration and development," *Fresenius Environmental Bulletin*, vol. 30, no. 64, pp. 6957–6964, 2021.

[21] Y. Zhao, X. Zhang, S. Zhang, J. Yang, X. Li, and S. Heng, "Multi-factor controls on initial gas production pressure of coalbed methane wells in Changzhi-Anze block, central-southern of Qinshui Basin, China," *Adsorption Science & Technology*, vol. 38, no. 1-2, pp. 3–23, 2020.

[22] J. Li, S. Tang, S. Zhang et al., "Characterization of unconventional reservoirs and continuous accumulations of natural gas in the Carboniferous-Permian strata, mid-eastern Qinshui basin, China," *Journal of Natural Gas Science and Engineering*, vol. 49, pp. 298–316, 2018.

[23] J. Shi, L. Zeng, X. Zhao, Y. Zhang, and J. Wang, "Characteristics of natural fractures in the upper Paleozoic coal bearing strata in the southern Qinshui Basin, China: implications for coalbed methane (CBM) development," *Marine and Petroleum Geology*, vol. 113, article 104152, 2020.

[24] D. Liu, Z. Zou, Y. Cai, Y. Qiu, Y. Zhou, and S. He, "An updated study on CH_4 isothermal adsorption and isosteric adsorption heat behaviors of variable rank coals," *Journal of Natural Gas Science and Engineering*, vol. 89, article 103899, 2021.

[25] Z. Zhang, Y. Qin, J. Bai, G. Li, X. Zhang, and X. Wang, "Hydrogeochemistry characteristics of produced waters from CBM wells in Southern Qinshui Basin and implications for CBM commingled development," *Journal of Natural Gas Science and Engineering*, vol. 56, pp. 428–443, 2018.

[26] A. Najibi, M. Ghafoori, G. Lashkaripour, and M. R. Asef, "Reservoir geomechanical modeling: in-situ stress, pore pressure, and mud design," *Journal of Petroleum Science and Engineering*, vol. 151, pp. 31–39, 2017.

[27] X. Kong, C. Zhang, G. Hu et al., "3D finite element simulation of in-situ stress and its application in coalbed methane exploration - a case study in southern Qinshui Basin," in *Proceedings of the International Field Exploration and Development Conference*, pp. 975–986, Chengdu, China, July 2020.

[28] E. Hoek and C. Martin, "Fracture initiation and propagation in intact rock - a review," *Journal of Rock Mechanics and Geotechnical Engineering*, vol. 6, no. 4, pp. 287–300, 2014.

[29] S. Saurabh and S. Harpalani, "Stress path with depletion in coalbed methane reservoirs and stress based permeability modeling," *International Journal of Coal Geology*, vol. 185, pp. 12–22, 2018.

[30] Z. Liu, D. Liu, Y. Cai, Y. Yao, Z. Pan, and Y. Zhou, "Application of nuclear magnetic resonance (NMR) in coalbed methane and shale reservoirs: a review," *International Journal of Coal Geology*, vol. 218, article 103261, 2020.

[31] K. Zhang, L. Wang, Y. Cheng et al., "Geological control of fold structure on gas occurrence and its implication for coalbed gas outburst: case study in the Qinan coal mine, Huaibei coalfield, China," *Natural Resources Research*, vol. 29, no. 2, pp. 1375–1395, 2020.